ELSEVIER

Helicity of the W boson in lepton + jets $t\bar{t}$ events

DØ Collaboration

V.M. Abazov [u], B. Abbott [bb], A. Abdesselam [k], M. Abolins [au], V. Abramov [x],
B.S. Acharya [q], D.L. Adams [az], M. Adams [ah], S.N. Ahmed [t], G.D. Alexeev [u], A. Alton [at],
G.A. Alves [b], Y. Arnoud [i], C. Avila [e], V.V. Babintsev [x], L. Babukhadia [ay], T.C. Bacon [z],
A. Baden [aq], S. Baffioni [j], B. Baldin [ag], P.W. Balm [s], S. Banerjee [q], E. Barberis [as],
P. Baringer [an], J. Barreto [b], J.F. Bartlett [ag], U. Bassler [l], D. Bauer [ak], A. Bean [an],
F. Beaudette [k], M. Begel [ax], A. Belyaev [af], S.B. Beri [o], G. Bernardi [l], I. Bertram [y],
A. Besson [i], R. Beuselinck [z], V.A. Bezzubov [x], P.C. Bhat [ag], V. Bhatnagar [o],
M. Bhattacharjee [ay], G. Blazey [ai], F. Blekman [s], S. Blessing [af], A. Boehnlein [ag],
N.I. Bojko [x], T.A. Bolton [ao], F. Borcherding [ag], K. Bos [s], T. Bose [aw], A. Brandt [bd],
G. Briskin [bc], R. Brock [au], G. Brooijmans [aw], A. Bross [ag], D. Buchholz [aj], M. Buehler [ah],
V. Buescher [n], V.S. Burtovoi [x], J.M. Butler [ar], F. Canelli [ax], W. Carvalho [c], D. Casey [au],
H. Castilla-Valdez [r], D. Chakraborty [ai], K.M. Chan [ax], S.V. Chekulaev [x], D.K. Cho [ax],
S. Choi [ae], S. Chopra [az], D. Claes [av], A.R. Clark [ab], B. Connolly [af], W.E. Cooper [ag],
D. Coppage [an], S. Crépé-Renaudin [i], M.A.C. Cummings [ai], D. Cutts [bc], H. da Motta [b],
G.A. Davis [ax], K. De [bd], S.J. de Jong [t], M. Demarteau [ag], R. Demina [ax], P. Demine [m],
D. Denisov [ag], S.P. Denisov [x], S. Desai [ay], H.T. Diehl [ag], M. Diesburg [ag], S. Doulas [as],
L.V. Dudko [w], L. Duflot [k], S.R. Dugad [q], A. Duperrin [j], A. Dyshkant [ai], D. Edmunds [au],
J. Ellison [ae], J.T. Eltzroth [bd], V.D. Elvira [ag], R. Engelmann [ay], S. Eno [aq], P. Ermolov [w],
O.V. Eroshin [x], J. Estrada [ax], H. Evans [aw], V.N. Evdokimov [x], T. Ferbel [ax], F. Filthaut [t],
H.E. Fisk [ag], M. Fortner [ai], H. Fox [n], S. Fu [aw], S. Fuess [ag], E. Gallas [ag], A.N. Galyaev [x],
M. Gao [aw], V. Gavrilov [v], K. Genser [ag], C.E. Gerber [ah], Y. Gershtein [bc], G. Ginther [ax],
B. Gómez [e], P.I. Goncharov [x], K. Gounder [ag], A. Goussiou [al], P.D. Grannis [ay],
H. Greenlee [ag], Z.D. Greenwood [ap], S. Grinstein [a], L. Groer [aw], S. Grünendahl [ag],
S.N. Gurzhiev [x], G. Gutierrez [ag], P. Gutierrez [bb], N.J. Hadley [aq], H. Haggerty [ag],
S. Hagopian [af], V. Hagopian [af], R.E. Hall [ac], C. Han [at], S. Hansen [ag], J.M. Hauptman [am],
C. Hebert [an], D. Hedin [ai], J.M. Heinmiller [ah], A.P. Heinson [ae], U. Heintz [ar],

M.D. Hildreth [al], R. Hirosky [bf], J.D. Hobbs [ay], B. Hoeneisen [h], J. Huang [ak], Y. Huang [at], I. Iashvili [ae], R. Illingworth [z], A.S. Ito [ag], M. Jaffré [k], S. Jain [bb], V. Jain [az], R. Jesik [z], K. Johns [aa], M. Johnson [ag], A. Jonckheere [ag], H. Jöstlein [ag], A. Juste [ag], W. Kahl [ao], S. Kahn [az], E. Kajfasz [j], A.M. Kalinin [u], D. Karmanov [w], D. Karmgard [al], R. Kehoe [au], S. Kesisoglou [bc], A. Khanov [ax], A. Kharchilava [al], B. Klima [ag], J.M. Kohli [o], A.V. Kostritskiy [x], J. Kotcher [az], B. Kothari [aw], A.V. Kozelov [x], E.A. Kozlovsky [x], J. Krane [am], M.R. Krishnaswamy [q], P. Krivkova [f], S. Krzywdzinski [ag], M. Kubantsev [ao], S. Kuleshov [v], Y. Kulik [ag], S. Kunori [aq], A. Kupco [g], V.E. Kuznetsov [ae], G. Landsberg [bc], W.M. Lee [af], A. Leflat [w], F. Lehner [ag,1], C. Leonidopoulos [aw], J. Li [bd], Q.Z. Li [ag], J.G.R. Lima [ai], D. Lincoln [ag], S.L. Linn [af], J. Linnemann [au], R. Lipton [ag], L. Lueking [ag], C. Lundstedt [av], C. Luo [ak], A.K.A. Maciel [ai], R.J. Madaras [ab], V.L. Malyshev [u], V. Manankov [w], H.S. Mao [d], T. Marshall [ak], M.I. Martin [ai], S.E.K. Mattingly [bc], A.A. Mayorov [x], R. McCarthy [ay], T. McMahon [ba], H.L. Melanson [ag], A. Melnitchouk [bc], M. Merkin [w], K.W. Merritt [ag], C. Miao [bc], H. Miettinen [be], D. Mihalcea [ai], N. Mokhov [ag], N.K. Mondal [q], H.E. Montgomery [ag], R.W. Moore [au], Y.D. Mutaf [ay], E. Nagy [j], M. Narain [ar], V.S. Narasimham [q], N.A. Naumann [t], H.A. Neal [at], J.P. Negret [e], S. Nelson [af], A. Nomerotski [ag], T. Nunnemann [ag], D. O'Neil [au], V. Oguri [c], N. Oshima [ag], P. Padley [be], N. Parashar [ap], R. Partridge [bc], N. Parua [ay], A. Patwa [ay], O. Peters [s], P. Pétroff [k], R. Piegaia [a], B.G. Pope [au], H.B. Prosper [af], S. Protopopescu [az], M.B. Przybycien [aj,2], J. Qian [at], A. Quadt [ax], S. Rajagopalan [az], P.A. Rapidis [ag], N.W. Reay [ao], S. Reucroft [as], M. Ridel [k], M. Rijssenbeek [ay], F. Rizatdinova [ao], T. Rockwell [au], C. Royon [m], P. Rubinov [ag], R. Ruchti [al], B.M. Sabirov [u], G. Sajot [i], A. Santoro [c], L. Sawyer [ap], R.D. Schamberger [ay], H. Schellman [aj], A. Schwartzman [a], E. Shabalina [ah], R.K. Shivpuri [p], D. Shpakov [as], M. Shupe [aa], R.A. Sidwell [ao], V. Simak [g], V. Sirotenko [ag], P. Slattery [ax], R.P. Smith [ag], G.R. Snow [av], J. Snow [ba], S. Snyder [az], J. Solomon [ah], Y. Song [bd], V. Sorín [a], M. Sosebee [bd], N. Sotnikova [w], K. Soustruznik [f], M. Souza [b], N.R. Stanton [ao], G. Steinbrück [aw], D. Stoker [ad], V. Stolin [v], A. Stone [ah], D.A. Stoyanova [x], M.A. Strang [bd], M. Strauss [bb], M. Strovink [ab], L. Stutte [ag], A. Sznajder [c], M. Talby [j], W. Taylor [ay], S. Tentindo-Repond [af], T.G. Trippe [ab], A.S. Turcot [az], P.M. Tuts [aw], R. Van Kooten [ak], V. Vaniev [x], N. Varelas [ah], F. Villeneuve-Seguier [j], A.A. Volkov [x], A.P. Vorobiev [x], H.D. Wahl [af], Z.-M. Wang [ay], J. Warchol [al], G. Watts [bg], M. Wayne [al], H. Weerts [au], A. White [bd], D. Whiteson [ab], D.A. Wijngaarden [t], S. Willis [ai], S.J. Wimpenny [ae], J. Womersley [ag], D.R. Wood [as], Q. Xu [at], R. Yamada [ag], T. Yasuda [ag], Y.A. Yatsunenko [u], K. Yip [az], J. Yu [bd], M. Zanabria [e], X. Zhang [bb], B. Zhou [at], Z. Zhou [am], M. Zielinski [ax], D. Zieminska [ak], A. Zieminski [ak], V. Zutshi [ai], E.G. Zverev [w], A. Zylberstejn [m]

[a] *Universidad de Buenos Aires, Buenos Aires, Argentina*
[b] *LAFEX, Centro Brasileiro de Pesquisas Físicas, Rio de Janeiro, Brazil*

[c] *Universidade do Estado do Rio de Janeiro, Rio de Janeiro, Brazil*
[d] *Institute of High Energy Physics, Beijing, People's Republic of China*
[e] *Universidad de los Andes, Bogotá, Colombia*
[f] *Charles University, Center for Particle Physics, Prague, Czech Republic*
[g] *Institute of Physics, Academy of Sciences, Center for Particle Physics, Prague, Czech Republic*
[h] *Universidad San Francisco de Quito, Quito, Ecuador*
[i] *Laboratoire de Physique Subatomique et de Cosmologie, IN2P3-CNRS, Universite de Grenoble 1, Grenoble, France*
[j] *CPPM, IN2P3-CNRS, Université de la Méditerranée, Marseille, France*
[k] *Laboratoire de l'Accélérateur Linéaire, IN2P3-CNRS, Orsay, France*
[l] *LPNHE, Universités Paris VI and VII, IN2P3-CNRS, Paris, France*
[m] *DAPNIA/Service de Physique des Particules, CEA, Saclay, France*
[n] *Universität Freiburg, Physikalisches Institut, Freiburg, Germany*
[o] *Panjab University, Chandigarh, India*
[p] *Delhi University, Delhi, India*
[q] *Tata Institute of Fundamental Research, Mumbai, India*
[r] *CINVESTAV, Mexico City, Mexico*
[s] *FOM-Institute NIKHEF and University of Amsterdam/NIKHEF, Amsterdam, The Netherlands*
[t] *University of Nijmegen/NIKHEF, Nijmegen, The Netherlands*
[u] *Joint Institute for Nuclear Research, Dubna, Russia*
[v] *Institute for Theoretical and Experimental Physics, Moscow, Russia*
[w] *Moscow State University, Moscow, Russia*
[x] *Institute for High Energy Physics, Protvino, Russia*
[y] *Lancaster University, Lancaster, United Kingdom*
[z] *Imperial College, London, United Kingdom*
[aa] *University of Arizona, Tucson, AZ 85721, USA*
[ab] *Lawrence Berkeley National Laboratory and University of California, Berkeley, CA 94720, USA*
[ac] *California State University, Fresno, CA 93740, USA*
[ad] *University of California, Irvine, CA 92697, USA*
[ae] *University of California, Riverside, CA 92521, USA*
[af] *Florida State University, Tallahassee, FL 32306, USA*
[ag] *Fermi National Accelerator Laboratory, Batavia, IL 60510, USA*
[ah] *University of Illinois at Chicago, Chicago, IL 60607, USA*
[ai] *Northern Illinois University, DeKalb, IL 60115, USA*
[aj] *Northwestern University, Evanston, IL 60208, USA*
[ak] *Indiana University, Bloomington, IN 47405, USA*
[al] *University of Notre Dame, Notre Dame, IN 46556, USA*
[am] *Iowa State University, Ames, IA 50011, USA*
[an] *University of Kansas, Lawrence, KS 66045, USA*
[ao] *Kansas State University, Manhattan, KS 66506, USA*
[ap] *Louisiana Tech University, Ruston, LA 71272, USA*
[aq] *University of Maryland, College Park, MD 20742, USA*
[ar] *Boston University, Boston, MA 02215, USA*
[as] *Northeastern University, Boston, MA 02115, USA*
[at] *University of Michigan, Ann Arbor, MI 48109, USA*
[au] *Michigan State University, East Lansing, MI 48824, USA*
[av] *University of Nebraska, Lincoln, NB 68588, USA*
[aw] *Columbia University, New York, NY 10027, USA*
[ax] *University of Rochester, Rochester, NY 14627, USA*
[ay] *State University of New York, Stony Brook, NY 11794, USA*
[az] *Brookhaven National Laboratory, Upton, NY 11973, USA*
[ba] *Langston University, Langston, OK 73050, USA*
[bb] *University of Oklahoma, Norman, OK 73019, USA*
[bc] *Brown University, Providence, RI 02912, USA*
[bd] *University of Texas, Arlington, TX 76019, USA*
[be] *Rice University, Houston, TX 77005, USA*
[bf] *University of Virginia, Charlottesville, VA 22901, USA*
[bg] *University of Washington, Seattle, WA 98195, USA*

Abstract

We examine properties of $t\bar{t}$ candidate events in lepton + jets final states to establish the helicities of W bosons in $t \to W + b$ decays. Our analysis is based on a direct calculation of a probability density for each event to correspond to a $t\bar{t}$ final state, as a function of the helicity of the W boson. Using the 125 events/pb of data collected by the DØ experiment at the Fermilab Tevatron $p\bar{p}$ Collider at $\sqrt{s} = 1.8$ TeV, we obtain a longitudinal helicity fraction $F_0 = 0.56 \pm 0.31$, consistent with the prediction of $F_0 = 0.70$ from the standard model.

The observation of the top quark at the Fermilab Tevatron [1,2] provides a new opportunity for examining detailed implications of the standard model (SM). In fact, the large mass of the top quark has led to speculation that its interactions might be especially sensitive to the mechanism of electroweak symmetry breaking and new physics that is expected to appear at the TeV energy scale. Several pioneering studies of production and decay of top quarks have already been published [3–5], and although these have been limited by the small size of the data sample of the 1992–1996 Run I of the Tevatron, they have indicated nevertheless that it is feasible to measure subtle properties of the top quark.

In this Letter, we report a measurement of the longitudinal component of the helicity of W bosons from $t \to Wb$ decays in $t\bar{t}$ candidate events. The helicity of the W boson (h_W) is reflected in the angular distribution of its decay products $l + \nu_l$, with $l = e$, μ, or two quarks (q, $\bar{q}'$). Our analysis is based on a method of extracting parameters that was particularly effective for the measurement of the mass of the top quark [6,7].

An important consequence of a heavy top quark is that, to good approximation, it decays as a free object. Its expected lifetime is $\approx 0.5 \times 10^{-24}$ s, and it therefore decays about an order of magnitude faster than the time needed to form bound states with other

E-mail address: canelli@fnal.gov (F. Canelli).

[1] Visitor from University of Zurich, Zurich, Switzerland.
[2] Visitor from Institute of Nuclear Physics, Krakow, Poland.

quarks [8]. Consequently, the spin information carried by top quarks is passed directly to their decay products, and the production and decay of $t\bar{t}$ provides a probe of the underlying dynamics, with minimal impact from gluon radiation and binding effects of QCD [8,9].

When averaged over top helicities, the decay of a top quark (spin $1/2$) to a W boson (spin 1) and a b quark (spin $1/2$), and the W boson to left-handed leptons or quarks (spin $1/2$), has the general form

$$\frac{3}{8} F_-(1 + \cos\hat{\phi})^2 + \frac{3}{4} F_0 (1 - \cos\hat{\phi}^2)$$
$$+ \frac{3}{8} F_+ (1 - \cos\hat{\phi})^2, \tag{1}$$

where $\hat{\phi}$ refers to the decay angle (l or d or s) relative to the b line of flight in the W rest frame, and F_-, F_0, and F_+ are the left-handed, longitudinal, and right-handed W-boson fractions, respectively. The emitted b quark is essentially massless compared to the top quark ($m_b \ll m_t$), and, in the context of the V–A charged-current weak interaction of the SM, to conserve angular momentum, the spin of the b quark, with its dominantly negative helicity (i.e., spin pointing opposite to its line of flight in the rest frame of the top quark) can therefore point either along or opposite to the spin of the top quark. In the first case, the projection of the spin of the W boson must vanish (i.e., the W is longitudinally polarized, or $h_W = 0$). If the spin of the b quark points opposite to the spin of the top quark, the W boson must then be left-hand polar-
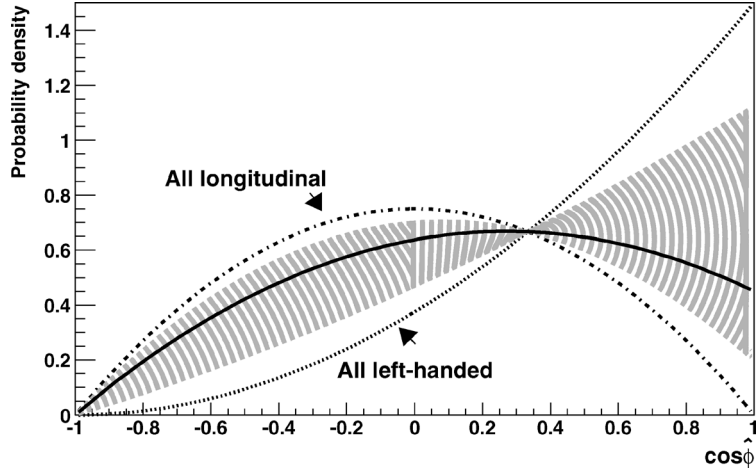
Fig. 1. The range of distributions in $\cos\hat{\phi}$ for different mixtures of left-handed and longitudinal W helicities. The dash-dotted line indicates the decay for purely longitudinal, and the dotted line for purely left-handed W bosons. The result of our analysis, shown by the grey region, corresponds to the most probable value of F_0 and its 68.3% interval (see later discussion). The black line is the prediction of the SM.

ized ($h_W = -1$). Hence, for massless b quarks, a top quark can decay only to a left-handed or a longitudinal W boson. Assuming $m_b = 0$, the V–A sector of the SM has $F_- = 2M_W^2/\kappa$, $F_0 = m_t^2/\kappa$, and $F_+ = 0$ (with $F_0 + F_- + F_+ = 1$, in general, defining κ). For a top-quark mass of $m_t = 174.3 \pm 5.1$ GeV/c^2 and W-boson mass $M_W = 80.4$ GeV/c^2 [10], the decay to longitudinal W bosons has a branching ratio of $F_0 = 0.70 \pm 0.01$. (The finite value $m_b \approx 4$ GeV/c^2 yields $F_+ \approx 0.7 m_b^2/\kappa$ and changes F_0 by $\approx -0.28 m_b^2/\kappa$.) There are possible scalar and tensor interactions that contribute differently than V–A to F_0 and F_-, but also have a very small F_+, again proportional to m_b^2 [11]. Given our limited statistics, we therefore set $F_+ = 0$, and in this analysis attempt to measure F_0. Fig. 1 shows the limiting forms of possible angular distributions in $\hat{\phi}$, assuming only left-handed and longitudinal contributions to W decay. To examine the nature of the tbW vertex, we use $t\bar{t}$ candidates observed at the DØ experiment [12] in $p\bar{p}$ collisions at a center-of-mass energy $\sqrt{s} = 1.8$ TeV. The data correspond to an integrated luminosity of 125 events/pb, and this analysis has the same lepton + jets sample that was used previously to extract the mass of the top quark [13]. That is, the signal is based on one of the W bosons decaying into $l + \nu_l$, and the other W to two quarks ($q\bar{q}'$); this leads to a final state characterized by one lepton and at least four jets (two from the fragmentation of the b quarks). F_0 is extracted by calculating for each

event a leading order (LO) probability density for its production and decay as $t\bar{t}$ [6,7]. This method offers increased statistical precision by using the decays of both W bosons.

An initial set of selection criteria involving pseudorapidities η, and transverse energies E_T of the lepton or jets, and the imbalance in transverse momentum in the event $\not{E}_T$ was used to improve the acceptance for lepton + jets from $t\bar{t}$ events relative to background [13]. These requirements were: $E_T^{\text{lepton}} > 20$ GeV, $|\eta_e| < 2$, $|\eta_\mu| < 1.7$, $E_T^{\text{jets}} > 15$ GeV, $|\eta_{\text{jets}}| < 2$, $\not{E}_T > 20$ GeV, $|E_T^{\text{lepton}}| + |\not{E}_T| > 60$ GeV, and $|\eta_W| < 2$ (calculated using the lepton, M_W, $\not{E}_T$, and the smaller value of the two solutions for the longitudinal momentum of the ν). A total of 91 events remained after imposing these requirements [13], and the present analysis uses only those that contain just four reconstructed jets (see below).

For a given value of F_0, the probability density for $t\bar{t}$ production and decay in the $e + $ jets final state is defined as

$$P_{t\bar{t}}(x; F_0) = \frac{1}{12\sigma_{t\bar{t}}} \int d\rho_1 \, dm_1^2 \, dM_1^2 \, dm_2^2 \, dM_2^2$$

$$\times \sum_{\text{perm}, \nu} \left| \mathcal{M}_{t\bar{t}}(F_0) \right|^2 \frac{f(q_1) f(q_2)}{|q_1||q_2|}$$

$$\times \Phi_6 W_{\text{jets}}(E_p, E_j), \qquad (2)$$

where x refers to the physical (measured) variables needed to characterize the final state, $|\mathcal{M}_{t\bar{t}}|^2 = \frac{g_s^2}{9}\mathcal{F}\bar{\mathcal{F}}(2 - \beta^2 s_{qt}^2)$ is the leading-order matrix element [14] for the process (neglecting $t\bar{t}$ spin correlations), where g_s is the strong coupling constant, β the speed of the top quark in the rest frame of the parton–parton collision, s_{qt} the sine of the angle between the momenta of the incident quark and the top quark, and $\mathcal{F}$ and $\bar{\mathcal{F}}$ containing the Breit–Wigners terms and the angular decays provided by Eq. (1), but with $F_+ = 0$, $f(q_1)$ and $f(q_2)$ are the CTEQ4M parton distribution functions (PDF) for the incident $p\bar{p}$ [15], Φ_6 is the phase-space factor for the 6-object final state, and $\sigma_{t\bar{t}}$ is the total cross section for $t\bar{t}$ production in LO. The sum is over all twelve permutations of jets (the effective permutation of the indistinguishable jets from the decay of the W is performed through a symmetrization of the matrix element) and all possible longitudinal momenta for neutrino solutions in W decay. The integration variables used in the calculation are the two top-quark invariant masses ($m_{1,2}$), the W boson invariant masses ($M_{1,2}$), and the energy of one of the quarks from W decay (ρ_1). Observed electron momenta are assumed to correspond to those of produced electrons. The angles of the jets are assumed to reflect the angles of the partons in the final state, and we ignore any transverse momentum for incident partons [7]. These assumptions, together with energy and momentum conservation, introduce 15 Dirac delta functions in the integration of the probability density, and reduce the dimensionality of the remaining integrations to the five given in Eq. (2). $W_{\text{jets}}(E_\text{p}, E_\text{j})$ corresponds to a function that parameterizes the mapping between parton-level energies E_p and jet energies measured in the detector E_j. This function includes the combined effects of radiation, hadronization, measurement resolution, and energy left outside of the jet-cone reconstruction algorithm. About 15 000 Monte Carlo (MC) $t\bar{t}$ events (generated with masses between 140 and 200 GeV/c^2 using HERWIG [16], and processed through the DØ detector-simulation package) were used to determine $W_{\text{jets}}(E_\text{p}, E_\text{j})$. For the $\mu + \text{jets}$ final state, W_{jets} is expanded to include the known muon momentum resolution, and an integration over muon momentum is added to Eq. (2).

All processes that contribute to the observed final state must be included in the probability density,

and the final probability density is therefore written as $P(x; F_0) = c_1 P_{t\bar{t}}(x; F_0) + c_2 P_{\text{bkg}}(x)$, where c_1 and c_2 are the signal and background fractions, and P_{bkg} refers to the production and decay probability density for background. $W + \text{jets}$ production corresponds to $\approx 80\%$ of the background, with the remaining 20% arising from multijet events where one jet mimics an electron. The VECBOS $W + \text{jets}$ matrix element [17] is used to calculate the background probability density, which is integrated over the energy of the four partons that lead to jets, and over the W-boson mass, and summed over the 24 jet permutations and two neutrino solutions. MC studies have shown that for multijet events the $W + \text{jets}$ probability density is much larger than that for $t\bar{t}$. Since all probabilities are added, we use the $W + \text{jets}$ probability density to represent the multijet background, and estimate a systematic uncertainty resulting from this assumption [7]. (Similarly, we ignore the $\approx 10\%$ contribution to $t\bar{t}$ production from gg fusion, and used only the $q\bar{q} \to t\bar{t}$ process in $\mathcal{M}_{t\bar{t}}$.) Effects such as geometric acceptance, trigger efficiencies, event selection, etc., are taken into account through a multiplicative function $A(x)$ that is independent of F_0. This function relates the $t\bar{t}$ and $W + \text{jets}$ probability densities to their respective measured probability densities $P_m(x; F_0) = A(x)[c_1 P_{t\bar{t}}(x; F_0) + c_2 P_{\text{bkg}}(x)]$. Because the calculation of the probability density involves a LO matrix element (valid only for four partons) for the production and decay process, we restrict the analysis to events with exactly four jets, reducing the data sample from 91 to 71 events. To increase the purity of signal, a selection is applied on the probability density of any event to correspond to background (P_{bkg}). This was done in Refs. [6,7] to minimize a bias introduced by the presence of background. The selected cutoff value of P_{bkg} is based on MC studies carried out before applying the method to data, and, for a top-quark mass of 175 GeV/c^2, it retains 71% of the signal and 30% of the background [6,7]. Fig. 2(a) shows a comparison between the probability for a background interpretation of events calculated for a large sample of MC events (upper-most histogram) and for the 71 $t\bar{t}$ candidates (data points). Only the 22 events to the left of the vertical line are chosen for the final analysis ($P_{\text{bkg}} < 10^{-11}$). The total number of MC events is normalized to the 71 4-jets $t\bar{t}$ candidates. The left-hatched (right-hatched) histogram shows the contri-
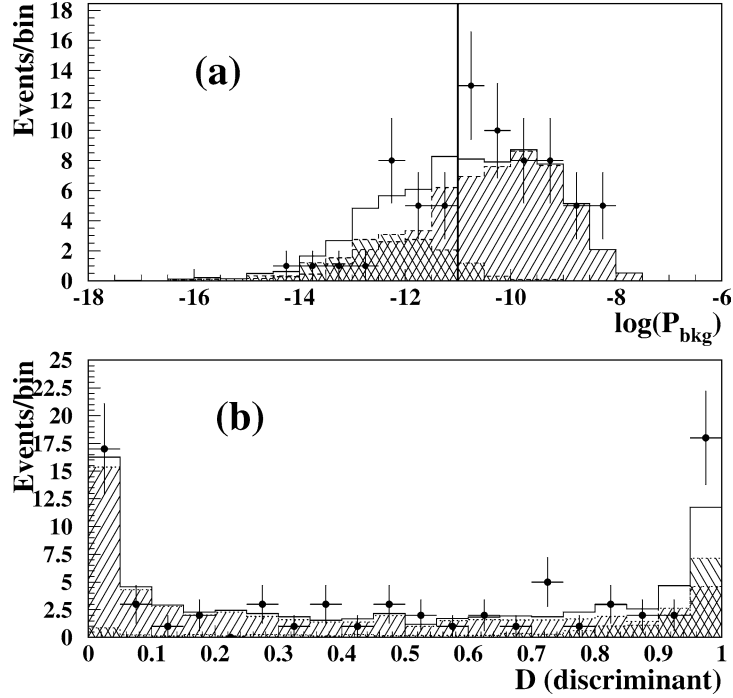
Fig. 2. (a) Distribution in probability of events being background, and (b) discriminant $P_{t\bar{t}}/(P_{t\bar{t}} + P_{\text{bkg}})$, calculated for 71 $t\bar{t}$ candidates (data points). The data are compared with results expected for the sum from MC-simulated sources of $t\bar{t}$ (left-hatched) and $W + 4$ jets (right-hatched) events. Only events with $P_{\text{bkg}} < 10^{-11}$ are considered in the final analysis.

bution from $t\bar{t}$ ($W + 4$ jets) MC events. The ratio of $t\bar{t}$ to $W + 4$ jets events in the MC is normalized to the 12/10 observed in data to the left of the vertical line ($S/B = 12/10$ is from the measurement in Ref. [6].) A discriminant $D = P_{t\bar{t}}/(P_{t\bar{t}} + P_{\text{bkg}})$ was defined to quantify the likelihood for an event to correspond to signal [13]. Fig. 2(b) shows D calculated as its most likely value with respect to the mass of the top quark for data (points with error bars) and for MC events (upper-most histograms), with the MC normalized as in Fig. 2(a). The discriminant is not used explicitly in this analysis, and is shown simply to illustrate the level of discrimination of signal and background. The above probability densities (P_m) are inserted into a likelihood function for $N = 22$ observed events. The $t\bar{t}$ probability density contains contributions from both F_0 and F_- helicities, and the ratio of F_0/F_- is allowed to vary. The best estimate of F_0 is obtained by maximizing the following likelihood with respect to F_0, subject to the constraint that F_0 must be physical, i.e., $0 \leqslant F_0 \leqslant 1$, and

$F_- + F_0 = 1$ [7]

$$L(F_0) = e^{-N \int P_m(x; F_0)\,\mathrm{d}x} \prod_{i=1}^{N} P_m(x_i; F_0), \qquad (3)$$

where, as before, P_m is the probability density in terms of observables for that event, and, inserting P_m into Eq. (3), the likelihood can be written as

$$-\ln L(F_0) = -\sum_{i=1}^{N} \ln\big[c_1 P_{t\bar{t}}(x_i; F_0) + c_2 P_{\text{bkg}}(x_i)\big]$$

$$+ N c_1 \int A(x) P_{t\bar{t}}(x; F_0)\,\mathrm{d}x$$

$$+ N c_2 \int A(x) P_{\text{bkg}}(x)\,\mathrm{d}x \qquad (4)$$

The above acceptance-correction integrals are evaluated using MC methods, where $A(x)$ takes the values 1 or 0, depending on whether the event is accepted or rejected. The best values of F_0 and the parameters c_i are obtained by minimizing $\ln L(F_0)$
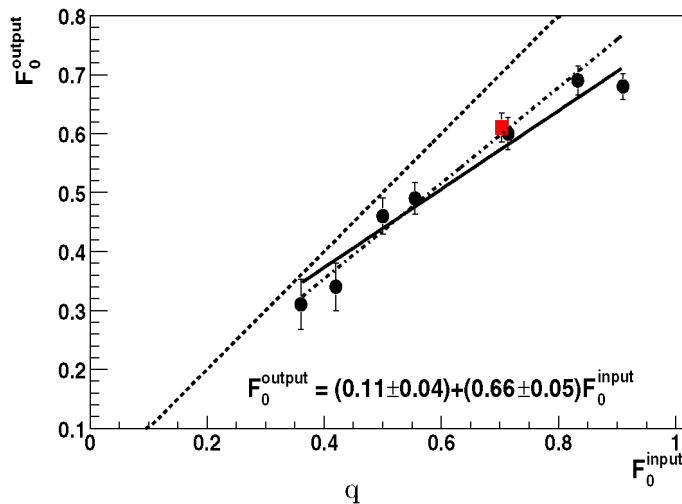
Fig. 3. Result of F_0 extraction (F_0^{output}) as a function of F_0^{input}, for ensembles of 12 $t\bar{t}$ signal and 10 $W+$ jets events for PYTHIA samples (black dots) and one HERWIG point (square), after all selections. The dotted line has unit slope and passes through $(0,0)$. The solid line is a fit to the results from PYTHIA that we use in the analysis. For comparison, the dot-dashed line is a fit obtained for high-statistic samples of PYTHIA events.

with respect to all three parameters. The response of the analysis (i.e., extracted F_0) to different input values of F_0 is examined by fluctuating the number of events according to a binomial distribution with an average of 12 events for signal (S) and 10 events for background (B). Results from analyzing such samples of PYTHIA MC [18] events (shown in Fig. 3) indicate that a response correction must be applied to the data. Studies using resolution-smeared partons (rather than jets) indicate that the reason the slope of the response correction differs from unity may originate from gluon radiation or jet misreconstruction, which is not included in our definition of probabilities in Eq. (2).

We apply the correction from Fig. 3 to $L(F_0)$ for our sample of 22 events, and the final results are shown in Fig. 4(a), along with a fifth-order polynomial fit to the final $L(F_0)$, which is used to characterize the results. For $m_t = 175$ GeV/c^2, we find the most likely $F_0 = 0.60 \pm 0.30$(stat), with a signal-to-background ratio that is compatible with the value of 0.54 found in the mass analysis [6].

When a probability density represents the data accurately, the maximum likelihood method provides an unbiased estimate of any parameter. Consequently, because the current uncertainty in m_t is sufficiently large to affect the value of F_0, the likelihood can be max-

imized as a function of two variables (F_0 and m_t), which would then take correct account of any correlation between the two parameters and the fact that F_0 is bounded between 0 and 1. Given our limited statistics, the best way to account for the uncertainty in m_t is to project the two-dimensional likelihood onto the F_0 axis, and obtain the systematic uncertainty on F_0 from the uncertainty on m_t, by integrating the probability over the mass, which we do from 165 to 190 GeV/c^2, in steps of 2.5 GeV/c^2, using no other prior knowledge (external input) for the mass. Fig. 5 shows $L(F_0, m_t)$ normalized by its maximum value, after applying the response correction from Fig. 3 to data. Fig. 4(b) shows $L(F_0)/L_{\max}$ from Fig. 5, after integration over m_t. The results in Fig. 4(b) are also fitted to a 5th-order polynomial as a function of F_0. We use the most probable output value (at the maximum) to define the extracted F_0. The uncertainty on F_0 (shaded region in Fig. 4(b)) is defined by half of the most narrow interval within which the integral of the normalized probability function contains 68.3% of the area, and reflects the statistical error convoluted with the uncertainty on m_t. Thus, we obtain $F_0 = 0.56 \pm 0.31$(stat & m_t). The uncertainty on m_t is the only one we are able to treat in this general manner.

To assess the impact of other uncertainties in F_0, the acceptance corrections were changed within their
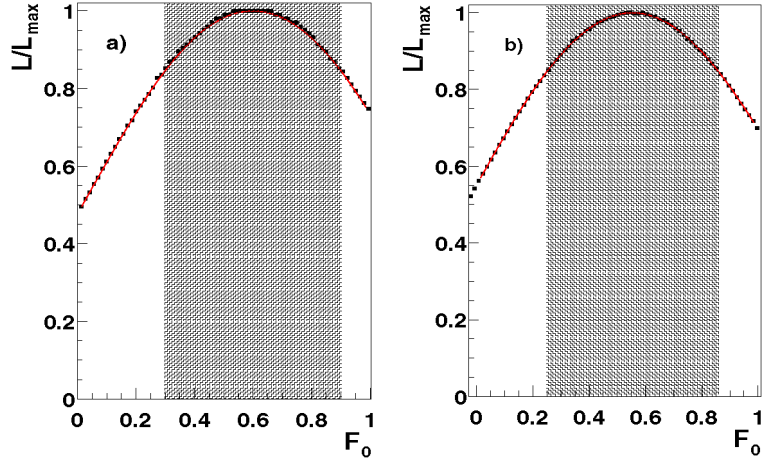
Fig. 4. (a) Likelihood normalized to its maximum value, as a function of F_0 for data from Run I. (b) Likelihood as a function of F_0, after integration over m_t (see text). The curves are 5th-order polynomials fitted to the likelihood. The hatched areas correspond to the most narrow 68.3% probability interval.
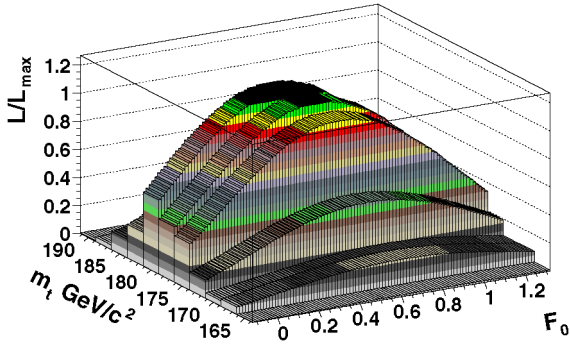

Fig. 5. Likelihood normalized to its maximum value as a function of m_t and F_0.

Table 1
Impact of systematic and statistical uncertainties on the measurement of F_0

Acceptance and response	0.055
Multijet background	0.024
Model for $t\bar{t}$ production	0.020
Multiple $p\bar{p}$ interactions	0.006
Jet energy scale	0.014
Parton distribution functions	0.008
Impact of spin correlations on $t\bar{t}$ events	0.008
Total systematic uncertainties, except for m_t	0.070
Statistics and uncertainty in m_t (see text)	0.306
Total uncertainty	0.314

uncertainties, the response recalculated, and F_0 remeasured in the data. The changes found in F_0 (rms) are then quoted as the systematic errors from acceptance and response. The analysis was also redone with and without considering multijet background events, using PYTHIA and HERWIG $t\bar{t}$ MC samples, with PYTHIA multiple $p\bar{p}$ interactions turned on and off. The resultant differences in F_0 were taken, respectively, as the systematic errors from multijet background, the $t\bar{t}$ model, and uncertainty from multiple $p\bar{p}$ interactions. The systematic errors from PDFs and jet energy scale were evaluated as in Ref. [6], but by studying the effect on F_0 instead of the top mass. Parton-level generators with and without spin correlations between the top and antitop quarks were used to

estimate the final systematic error in Table 1. Adding all the systematic errors in Table 1 in quadratures, we obtain $F_0 = 0.56 \pm 0.31(\text{stat} \& m_t) \pm 0.07(\text{sys})$. Combining the two errors in quadrature, we get $F_0 = 0.56 \pm 0.31$, which is consistent with expectations of the SM, as well as with the measurement from the CDF Collaboration of 0.91 ± 0.39 [3]. The grey region in Fig. 1 shows our result in terms of the 68.3% probability interval of our measured value of F_0 as a function of $\hat{\phi}$. The black curve represents the expectation for the V–A sector of the SM, and the limits of the distributions in $\hat{\phi}$ are shown by the dotted line (pure $h_W = -1$) and dot-dashed line (pure $h_W = 0$). In summary, we have extracted a longitudinal-helicity fraction of 0.56 ± 0.31 for W boson decays in lepton + jets channels in $t\bar{t}$ events. Although our

measurement is limited by the small event sample of Run I, this powerful technique should provide far greater sensitivity to any departures from the SM in the far larger data sample anticipated in the current Run II.

Acknowledgements

References

[1] DØ Collaboration, S. Abachi, et al., Phys. Rev. Lett. 74 (1995) 2632.
[2] CDF Collaboration, F. Abe, et al., Phys. Rev. Lett. 74 (1995) 2626.
[3] CDF Collaboration, T. Affolder, et al., Phys. Rev. Lett. 84 (2000) 216.
[4] DØ Collaboration, B. Abbott, et al., Phys. Rev. Lett. 85 (2000) 256.
[5] CDF Collaboration, D. Acosta, et al., Phys. Rev. D 71 (2005) 031101.
[6] DØ Collaboration, V.M. Abazov, et al., Nature 429 (2004) 638.
[7] M.F. Canelli, PhD thesis, University of Rochester, 2003; J.C. Estrada, PhD thesis, University of Rochester, 2001.
[8] I. Bigi, Y. Dokshitzer, V. Khoze, J. Kuhn, P. Zerwas, Phys. Lett. B 181 (1986) 157.
[9] M. Fischer, S. Groote, J.G. Korner, M.C. Mauser, Phys. Rev. D 65 (2002) 54036.
[10] Particle Data Group, K. Hagiwara, et al., Phys. Rev. D 66 (2002) 010001.
[11] C.A. Nelson, B.T. Kress, M. Lopes, T.P. McCauley, Phys. Rev. D 56 (1997) 5928.
[12] DØ Collaboration, S. Abachi, et al., Nucl. Instrum. Methods A 338 (1994) 185.
[13] DØ Collaboration, B. Abbott, et al., Phys. Rev. D 58 (1998) 052001.
[14] G. Mahlon, S. Parke, Phys. Rev. Lett. B 411 (1997) 133.
[15] CTEQ Collaboration, H.L. Lai, et al., Phys. Rev. D 51 (1995) 4763.
[16] G. Marchesini, et al., Comput. Phys. Commun. 67 (1992) 467.
[17] F.A. Berends, H. Kuijf, B. Tausk, W.T. Giele, Nucl. Phys. B 357 (1991) 32.
[18] T. Sjostrand, et al., Comput. Phys. Commun. 135 (2001) 238.